Available online at www.sciencedirect.com
SCIENCE DIRECT®
Catalysis Today 85 (2003) 311–320
CATALYSIS TODAY
www.elsevier.com/locate/cattod

The reactions of formaldehyde over the surfaces of uranium oxides. A comparative study between polycrystalline and single crystal materials

S.D. Senanayake, S.V. Chong[1], H. Idriss*

Department of Chemistry, The University of Auckland, Private Bag 92019, Auckland, New Zealand

Received 19 February 2003; accepted 4 March 2003

Abstract

The reaction of formaldehyde has been studied on the surfaces of UO_2(1 1 1) single crystal and polycrystalline UO_2. Most of adsorbed formaldehyde on the single crystal at room temperature reacted to give ethylene during TPD. On the polycrystalline surface, IR analyses showed that the main species present in the 88–200 K temperature domain are poly- and dioxymethylene. These species are mainly converted to stable formates that decompose at high temperature (above 550 K). The apparent activation energy for the reaction of the oxymethylenic species to formates in the 250–450 K region (calculated from the intensity of the ν_a COO IR band of formates, at 1575 cm^{-1}) is found equal to 12 kJ/mol. Overall, both surfaces (single crystal and polycrystalline) give qualitatively the same products, with the exception of formation of traces of methyl formate in the case of powder. However, the single crystal is far more active for the reductive coupling of formaldehyde to ethylene than the polycrystalline material. The difference in reaction selectivity between the single crystal and powder work is attributed to the method of preparation of the polycrystalline UO_2 material (made by H_2-reduction of α-U_3O_8) rather than to an intrinsic difference between both materials.

Keywords: Polycrystalline UO_2; H_2-reduction; Stable formates; UO_2(1 1 1) single crystals; Formaldehyde-infrared

1. Introduction

The reaction of small organic molecules with the surface of uranium oxides is of importance for several fundamental and applied reasons: (1) because large amounts of nuclear fuel are stored in water that ultimately contains organic molecules [1]; (2) probing into the actinide elements (f-orbitals [2]) may trigger other reaction pathways for simple organic molecules not encountered by the early transition metals (such as making of furan from C2 compounds [3] and tetramerisation of CO to enedionediolates [2]); (3) the uranium oxide system, one of the richest systems with over 30 different crystallographic phases, depending on the O/U ratio and preparation conditions, lends itself naturally to oxidation/reduction reactions [4].

The reactions of formaldehyde have been investigated over several polycrystalline and single crystal oxides surfaces. These include TiO_2 [5,6], V–Ti oxides [7], ZnO [8], $ZnAl_2O_4$ [8], Cu–ZnO–Al_2O_3 [9], ThO_2 [10], and CeO_2 [11] by several groups. Several reactions were identified depending on the nature and

* Corresponding author. Fax: +64-9-373-7422.
E-mail address: h.idriss@auckland.ac.nz (H. Idriss).
[1] Present address: Materials Technologies Group, Industrial Research Limited, P.O. Box 31-310, Lower Hutt, New Zealand.

0920-5861/$ – see front matter © 2003 Published by Elsevier B.V.
doi:10.1016/S0920-5861(03)00397-3

prior treatment of the oxide: reduction to methanol, oxidation to formic acid, decomposition to CO/CO_2 and H_2/H_2O, dimerisation to methylformate (Tishchenko reaction [12]), reaction with CO/H_2 to ethylene glycol on Rh_2O_3 [13], reductive coupling to ethylene on TiO_2 [14] and CO insertion to coordinated diols [15]. Two land mark articles treating the reaction of formaldehyde on oxides deserve particular attention. The first (Busca et al. [10]) treated the vibrational frequency of species resulting from the adsorption of formaldehyde over a variety of oxides (Al_2O_3, ThO_2, ZrO_2, TiO_2, MgO, and Fe_2O_3) while the second (Ai [12]) focused on the catalytic reaction. The main observed species on most of the oxides were formates [10], and the main reaction product was methylformate [12]. It is also worth reminding of the pioneering work of Tanabe and Saito on a series of alkali oxides [16] and the interesting correlation between the oxide activity to ester formation from aldehydes and the basicity of the oxides.

In this work, the reaction of formaldehyde is studied on UO_2(1 1 1) single crystal and on UO_2 powder for the following two reasons. First, to compare the reaction of the (1 1 1) oriented UO_2 single crystal (the (1 1 1) surface is the most stable surface of the fluorite structure [17]) to that of the polycrystalline. Second, to study the evolution of the adsorbed species by IR as a function of temperature. The single crystal study was conducted by low energy electron diffraction intensity versus time (LEED *I–T*) experiment and TPD, while the polycrystalline study was conducted by TPD and IR.

2. Experimental

2.1. UO_2(1 1 1) single crystal

A stainless steel ultra high vacuum (UHV) chamber was used for both temperature programmed desorption (TPD) and adsorption measurements. It was pumped by a 1200 L/s Varian diffusion pump, a titanium sublimation pump, and 270 L/s Perkin-Elmer ion pump, at base pressure of less than 1.33×10^{-10} kPa. The system contained an OCI Vacuum Microengineering four-grid LEED/AES optics, a Hiden quadrupole mass spectrometer, an argon ion sputter gun, and a molecular beam source region.

A 1 mm thick UO_2(1 1 1) single crystal with $\sim$20 mm^2 area was used in all experiments. The UO_2(1 1 1) single crystal mount was published previously [18]. Surface cleanliness and stoichiometry were checked by LEED and AES prior to experiments.

The dosing of formaldehyde (by decomposition of paraformaldehyde) for TPD experiments was carried out by positioning the crystal in front of the dosing needle, which gave a gain of $\sim$3.3 times compared to the back filling method. A heating rate of 0.90 ± 0.05 K/s was used in all the TPD experiments through a calibrated power supply.

2.2. Quantitative analysis of TPD peaks

Due to mass spectrometer sensitivity TPD peaks areas must be corrected. These correction factors are calculated following the method of Ko et al. [19]. All TPD spectra presented are in their raw form without smoothing. The areas of the peaks in the TPD were calculated with the trapezoid rule, a mathematical integral method used to calculate the total area under many data points. The area of the peak was subtracted from the background of the chamber. The computed correction factors relative to CO are as follows—formaldehyde: m/z 30 = 3.41; CO_2: m/z 44 = 1.34; ethylene: m/z 27 = 3.55; and methanol: m/z 31 = 2.17.

2.3. Sticking coefficient determination

The adsorption of formaldehyde on the surface of UO_2(1 1 1) single crystal was investigated through LEED intensity versus time (*I–T*) experiment by assuming that the decrease in intensity of the diffraction spot is proportional to the number of adsorbates [20] LEED image of this single crystal is shown in Fig. 1. The experimental set-up involved a computer interfaced digital camera (Hitachi) mounted on the viewport of a back-displayed OCI Vacuum Microengineering four-grid LEED/AES optics, with the data acquisition of the LEED diffraction spot intensity measurement performed by the SMARTLEED software from VG Microtech. The Van der Waals radius of formaldehyde is close to 2.05 Å, while the distance between two U atoms (or two O atoms) along the (1 1 1) surface is 3.87 Å. It is thus reasonable to assume that total coverage will be obtained with a

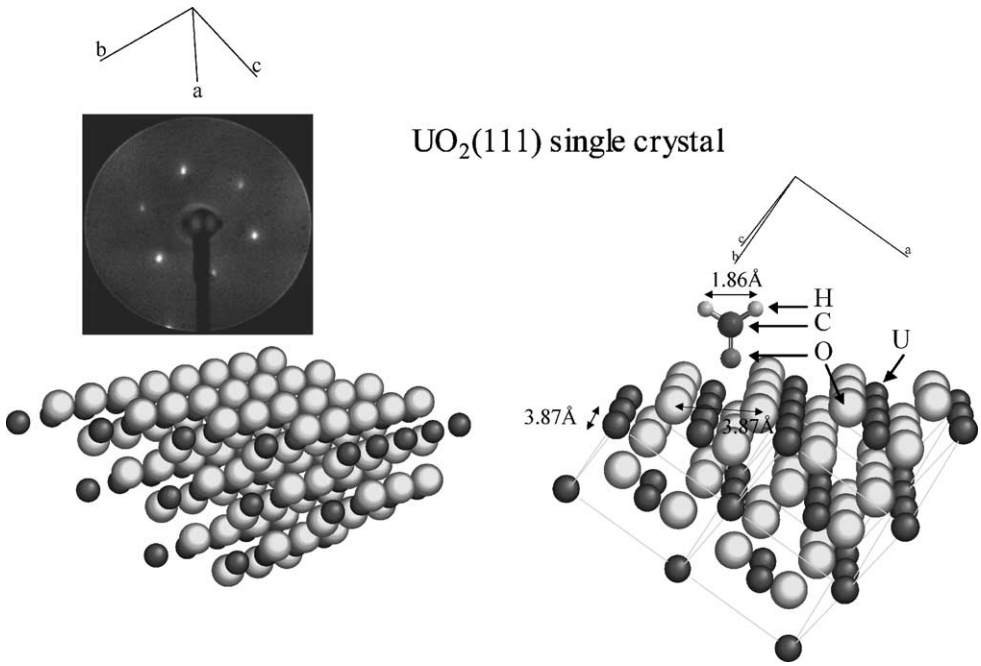

Fig. 1. LEED pattern of UO_2(1 1 1) single crystal. Also shown two representations of the (1 1 1) fluorite surface (rotated by 90°) to show the hexagonal pattern (axis *a* to the plane of the page) and a formaldehyde molecule close to the surface (atoms of HCHO are not drawn with the same surface atomic scale).

HCHO to U ratio equal to 1. By first normalizing the *I–T* curve with respect to the total U cation sites, 7.71×10^{14} atoms/cm^2, on the surface (and assuming coverage $\theta = 0$ before formaldehyde exposure and $\theta = 1$ when the curve reached a plateau), the sticking coefficient, *s*, can be determined via the expression, $s = (\mathrm{d}n/\mathrm{d}t)/\text{flux}$, where the flux (molecules per cm^2 per second) is expressed as $P/\sqrt{2\pi mkT_g}$ or more generally equals $2.63 \times 10^{24} P/\sqrt{T_g M}$ (P in Pa, T_g in K and M in g mol^{-1}). For the adsorption of formaldehyde on UO_2(1 1 1) single crystal, the *I–T* experiment was conducted at 108.3 eV incident beam energy with a beam current of ~1.35 μA at 300 K. LEED diffraction spot intensity measurement was acquired at every 10 s interval, and a calibrated chart recorder was used to record the formaldehyde exposure pressure during the *I–T* experiment.

2.4. Polycrystalline UO_2

Polycrystalline UO_2 was prepared by H_2-reduction of α-U_3O_8 as previously reported [20]. The TPD and IR set-up are described elsewhere [21–23]. TPD peaks are manipulated as described above. All IR spectra are subtracted from the fresh UO_2 sample.

3. Results

3.1. UO_2(1 1 1) single crystal

Fig. 2 shows the results of the LEED *I–T* experiments for the calculation of the sticking probability following the method described in the experimental section. No integral order diffraction LEED pattern was observed at any stage of the *I–T* measurements. The sticking probabilities at $\theta = 0.15$ and $\theta = 0.5$ were 0.14 ± 0.02 and 0.05 ± 0.01, respectively. This is almost four times smaller than that of formic acid [24] on the same surface, and in accord with the low sticking probability of aldehydes (less polar) when compared to their carboxylic acids counterpart, on polar surfaces in general.

Fig. 3 presents the product distribution during TPD after 103.5 L HCHO adsorption at room temperature, while Table 1 presents the relative yields and peak

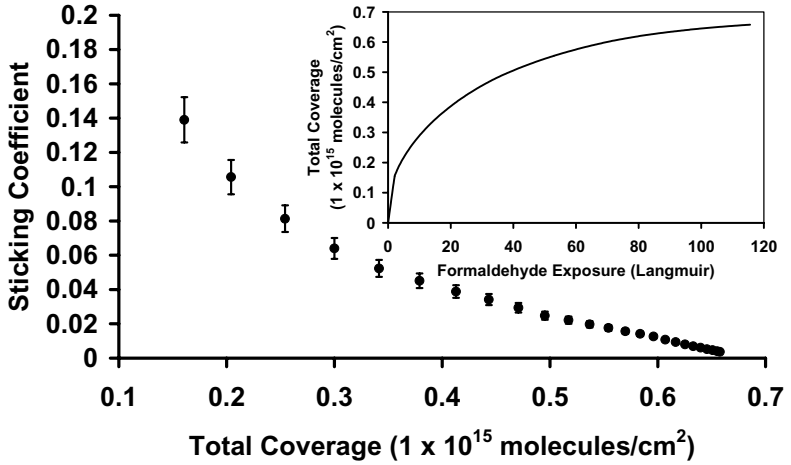

Fig. 2. LEED-extracted sticking coefficient (*s*) of HCHO on UO_2(1 1 1) at 300 K, as a function of total coverage. The inset shows surface coverage as a function of HCHO exposure.

temperature of these products. A weak desorption profile of un-reacted HCHO is seen at 350 K. The coincident desorption of *m*/*z* 28, 27 and 26 at 400 and 450 K indicates that these fragments are due to CH_2=CH_2. Small amounts of methanol are also seen in two peaks (≈400 and 500 K). While the desorption of the 400 K peak is coincident with that of formaldehyde, that at 500 K indicates that some stable methoxide species are present on the surface. The presence of both methanol and ethylene is due to reduction reactions occurring on the surface while CO and CO_2 are most likely due to decomposition of formate (formed from the oxidation of HCHO) to CO_2 and CO. H_2 and H_2O could not be accurately monitored due to their relatively small desorption. TPD was also conducted after several dosing increments, at low dosing <10 L no resolvable peaks other than HCHO were observed while increasing the dosing above 100 L did not result in observable changes in the relative yields, within experimental errors.

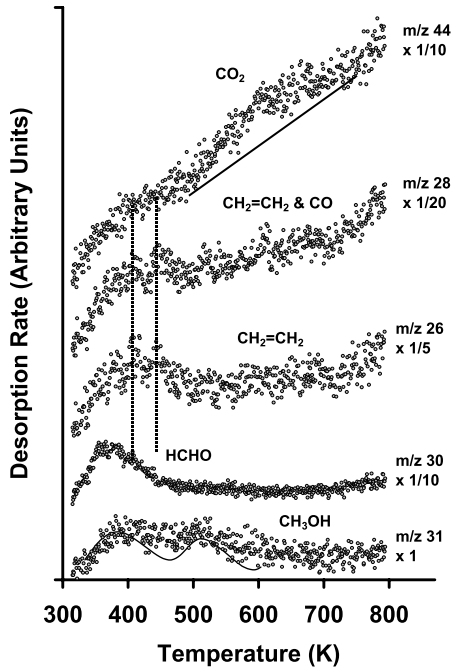

Fig. 3. TPD after HCHO (ca. 100 L) on UO_2(1 1 1) single crystal at 300 K.

3.2. Polycrystalline UO_2

Both XPS and XRD have confirmed that the cubic fluorite phase of UO_2 is obtained by hydrogen

Table 1
Product desorption during HCHO over UO_2(1 1 1) single crystal

Products/reactant	Peak temperature (K)	Selectivity	Relative yield
HCHO (*m*/*z* 30)	350	–	1.00
CH_2=H_2 (*m*/*z* 26)	400, 450	0.87	6.52
CO (*m*/*z* 28)	600	Traces	Traces
CH_3OH (*m*/*z* 31)	≈400, 500	0.03	0.04
CO_2 (*m*/*z* 28)	≈600	0.10	0.21

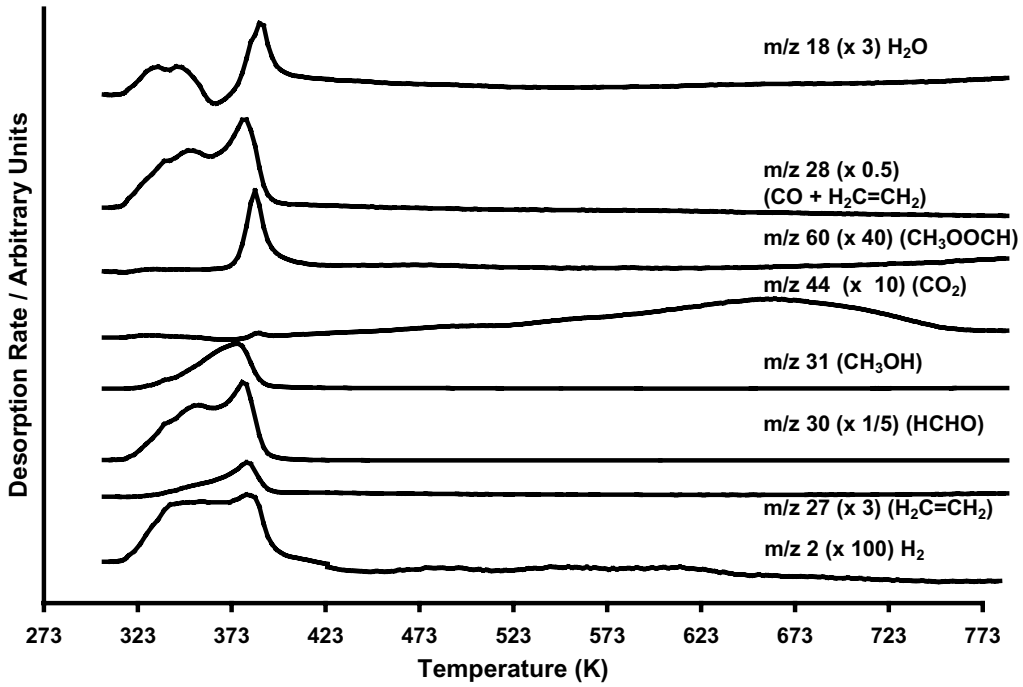

Fig. 4. TPD after HCHO (surface saturation) on polycrystalline UO_2(1 1 1) at 300 K.

reduction of α-U_3O_8 (orthorhombic) for 12 h at 101–33 kPa [21]. Fig. 4 shows TPD following formaldehyde adsorption on UO_2 powder at 300 K and the quantitative analyses are given in Table 2. Two well-resolved peaks for formaldehyde desorption are seen at 355 and 385 K. Only traces of H_2 desorb with the first peak. The second formaldehyde peak desorbs with other reaction products: ethylene, methanol and methylformate (small desorption of CO_2 is also seen). It is interesting to note the symmetry of the methylformate desorption, an indication of the expected second order desorption. The first order shape of the methanol peak indicates that it is a desorption limited process, i.e. methanol is most likely formed upon dosing (due to the reaction of formaldehyde with surface hydrogen left after the reduction process). Unlike the single crystal case relatively large amounts of CO_2 are seen at high temperature (a large peak centered at ≈600 K). The main difference with the single crystal results, however, is that of the formation of methylformate in the case of the powder. This is most likely due to pressure effects (and not intrinsic to the polycrystalline material). While powder TPD is conducted at 1.33×10^{-2} kPa that of single crystal is below 1.33×10^{-10} kPa and is thus less favorable for recombination reactions.

Table 2
Product desorption during HCHO over polycrystalline UO_2(1 1 1)

Products/reactant	Peak temperature (K)	Selectivity	Relative yield
HCHO	340–350, 380	–	1.00
CH_2=H_2	380	0.16	0.01
Methylformate	385	0.08	0.005
CH_3OH	380	0.59	0.04
CO_2	≈600	0.13	0.008
H_2	300–400	0.03	0.002

Fig. 5 shows IR of formaldehyde-adsorbed UO_2 powder at 88 K with the insert showing the increase in the IR signal as a function of exposure. Fig. 6 shows the effect of heating the dosed surface to increment temperature up to 650 K, while Fig. 7 presents the intensity of the main IR peaks of Fig. 6 as a function of temperature.

Upon dosing of HCHO at 88 K bands at 1128, 1040, 975 and 950 cm^{-1} are seen (Fig. 5). Heating

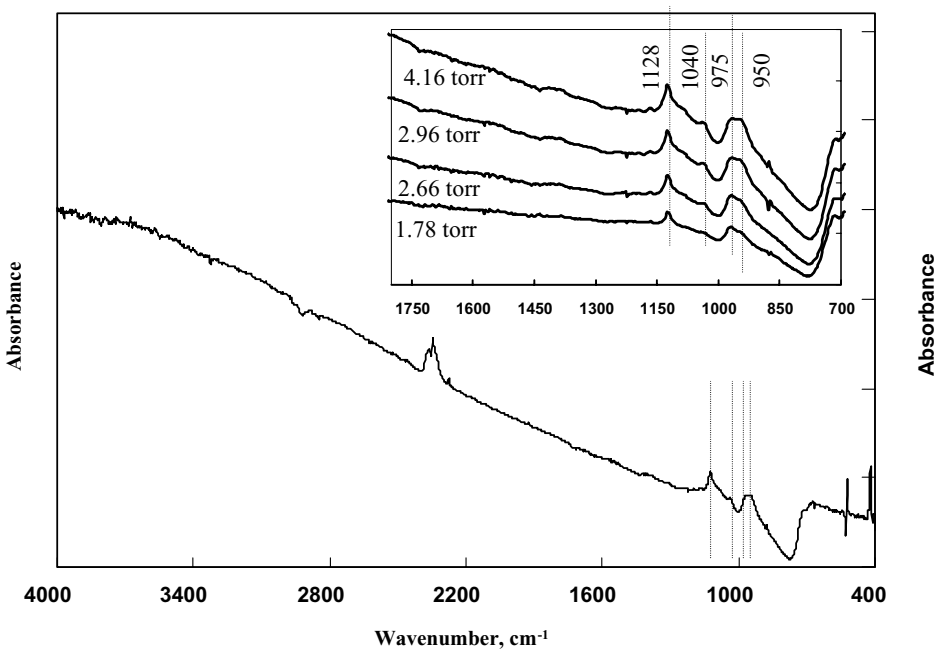

Fig. 5. IR bands observed upon HCHO adsorption on polycrystalline UO_2 at 88 K at different exposure.

to 183 K changed the relative intensity and position of these bands. The bands at 975 and 950 cm^{-1} shift to 943 and 912 cm^{-1} and a band at 1240 cm^{-1} appears. These bands decrease with heating and bands attributed to formate species emerge; clearly from 328 K and are dominant by 532 K. Formates start to decompose by 473 K and sharply decrease in intensity at 693 K. In order to analyse the data in Figs. 5 and 6, Table 3 has been constructed from results of other workers. In Table 3 the IR bands of gas-phase HCHO are presented [25], also shown bands for adsorbed formaldehyde in η^1 (80 K) and η^2 (250 K) configurations on Ru(0 0 1)–$p(2 \times 2)$O [25] single crystal, bands of adsorbed HCHO on Mo(1 1 0) single crystal [26] at 200 K, bands of paraformaldehyde [27], and bands attributed to dioxymethylene formed from HCHO on ThO_2 at 240 K [10].

The absence of the band at 1745 cm^{-1} clearly indicates that HCHO is not present in η^1 configuration. Most of the formaldehyde is present in a polyoxymethylene and dioxymethylene form. The band at 975 cm^{-1} has been observed by other workers on

Table 3
IR bands following adsorption of HCHO over several oxides

Assignment	HCHO gas-phase [25]	Polyoxymethylene [27], $(CH_2O)_n$	Dioxymethylene ThO_2 [10], (O_sCH_2O)	η^1 HCHO Ru(1 1 1)–O [26], $H_2CO_{(a)}$	η^2 HCHO Ru(1 1 1)–O [26], $H_2C_{(a)}O_{(a)}$	HCHO Pd(1 1 1) [37]	HCHO UO_2 (80 K) this work	HCHO UO_2 (183 K +) this work
νCO	1746		1070	1660–1680	980	1695	975	
ν_a(OCO)		1097				1120	1128	1125
ν_s(OCO)		932				945	950	943
$\rho(CH_2)$	1249	903	920	1195–1240	840	885	nr	912, 1240
$\omega(CH_2)$	1167	1381	1405, 1410 (V–Ti–O) [7]	–	1160	–		1178
$\delta(CH_2)$	1500	1508	1495, 1478 (V–Ti–O) [7]	1465	1450	–		–

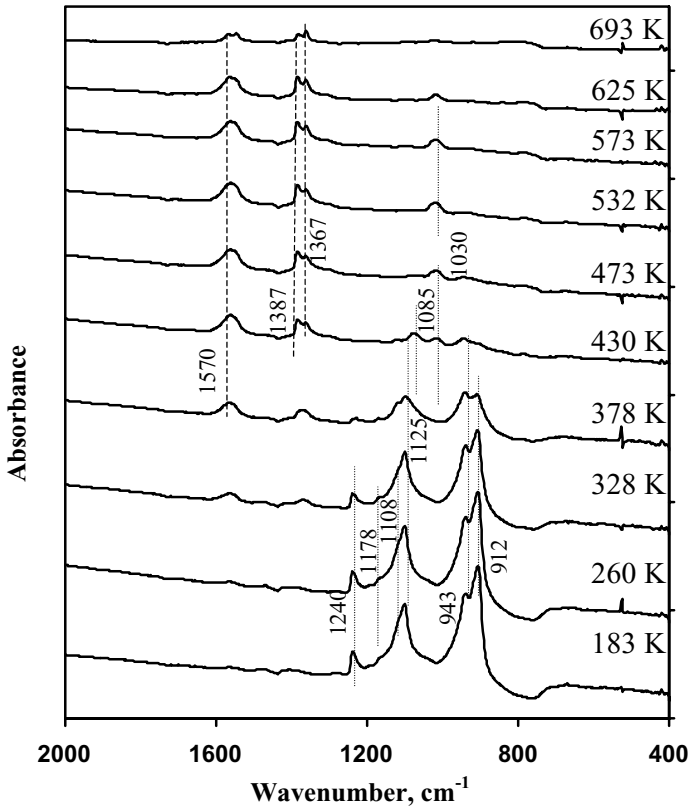

Fig. 6. Effect of increment temperature on the IR bands (of Fig. 5) following HCHO adsorption on polycrystalline UO_2.

Mo(1 1 1) from formaldehyde (at 980 cm^{-1}) but was not assigned. This band is unstable since it disappears by 183 K. Based on results of HCHO on Ru(1 1 1)–O it is tentatively attributed to η^2 HCHO that react to give some methoxides.

Upon heating, bands attributed to formate species are clear. ν_a(COO) at 1570 cm^{-1}, ν_s(COO) at 1367 cm^{-1} and δ(C–H) at 1387 cm^{-1}. These bands are very similar to those reported upon dosing of formic acid over polycrystalline UO_2 [42]. The separation between ν_a and ν_s of $\approx$200 cm^{-1} indicates that formates are in a chelating mode and not in a uni-dentate mode (bridging configuration is highly unlikely because the U–U distance is far larger than the distance between the two O atoms of the carboxylate group (ca. 2 Å): the shortest distance is 3.87 Å for the (1 1 1), (1 1 0), and (0 1 1) surfaces of the fluorite structure). A band at 1085 cm^{-1} appears upon heating to 430 K and follows formate species. TPD has shown that by this temperature methanol has desorbed. This band is thus not assigned to ν(OC) of methoxides. The out of plane C–H deformation of formic acid on Ag{1 1 1} has been seen at 1078 cm^{-1} and that of formate on the same surface at 1050 cm^{-1} [28]. Over CeO_2(1 1 1) single crystal this out of plane deformation mode was seen at 1055 cm^{-1} [29] and that of HCOONa at 1078 cm^{-1} [30]. A similar band (although at 1025 cm^{-1}) was observed upon dosing of HCOOH over polycrystalline UO_2 [42]. The appearance and disappearance of this band with those of ν_a and ν_s of the COO bands tend to assign it to out plane deformation of formates.

4. Discussion

The most stable surface of the fluorite structure is the [1 1 1] oriented. The surface is O terminated followed by an all U atoms layer and then followed by

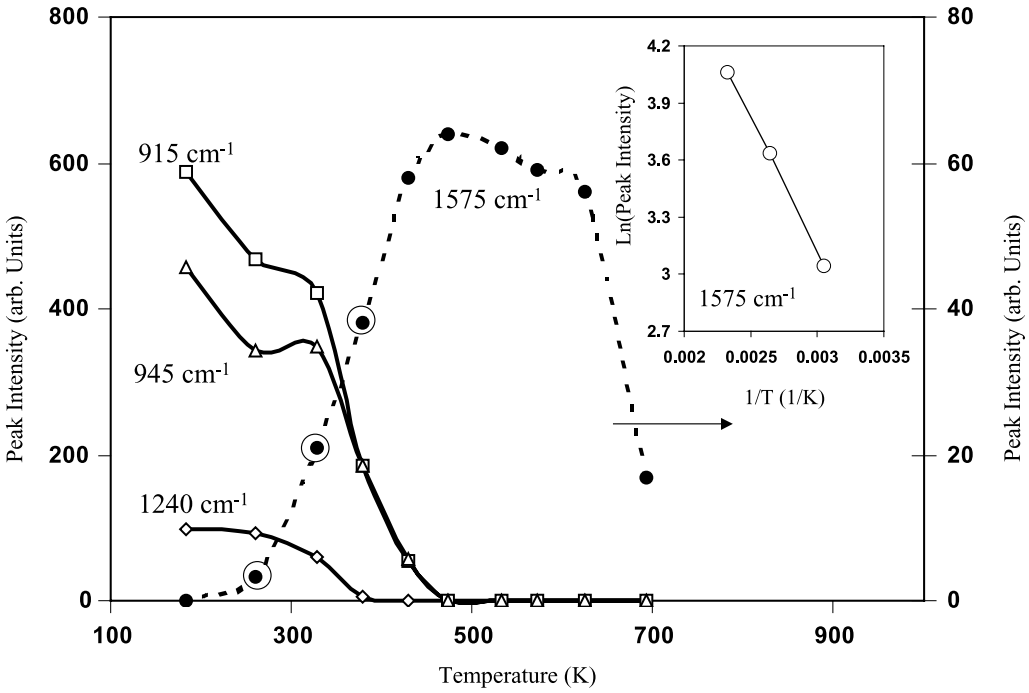

Fig. 7. Change of main peaks intensities of Fig. 6 as a function of temperature. The inset shows $\ln(\nu_a COO)$ of formates as function of $1/T$.

an all O layer, the U–U is 3.87 Å. Table 4 shows some properties of the surface of UO_2 with a comparison to CeO_2 (also a fluorite) together with main TPD results. Although the reaction of C1 and C2 carboxylic acids was investigated over CeO_2(1 1 1) no work has addressed the reactions of aldehydes yet on the surface of other well-defined fluorites. Both CeO_2(1 1 1) and UO_2(1 1 1) surfaces have very similar properties. Both surfaces have some mild reduction effect on formic acid; formation of few % of formaldehyde. TPD results comparing the reaction of formaldehyde and formic acid over single crystal and powder UO_2 are also shown in Table 4. A very good similarity is noticed with the exception of ethylene formation on the single crystal and of methylformate formation on the powder. Ethylene yield is far higher on the single crystal and this is most likely due to the method of making UO_2 powder rather than an intrinsic difference. UO_2 powder is made by H_2-reduction of α-U_3O_8 and this leaves large amounts of H atoms on the

Table 4
Comparison between some surface and bulk properties of CeO_2 and UO_2 and their surface reactivity

	UO_2(1 1 1) single crystal	UO_2 polycrystalline	CeO_2(1 1 1) single crystal
Surface energy (J/m^2)—relaxed	1.069 (Ref. [17])		1.195 (Ref. [38])
Bulk defect equilibrium (eV)		9.8 (Ref. [39])	6.58[a] (Ref. [38])
Bulk $E_{(M^{4+}-O^{2-})}$ (eV)		9.7[b]	10.0[b]
$V_{Mad}(O^{2-})$ (eV), $V_{Mad}(M^{4+})$ (eV)		21.4–39.9 (Ref. [40])	21.7–40.3 (Ref. [41])
HCOOH/TPD	Reduction to HCHO 1.4%, $CO/CO_2 = 1.21$ (Ref. [24])	Reduction to HCHO 3%, $CO/CO_2 = 1.43$ (Ref. [42])	Yield of HCHO 4.1%, $CO/CO_2 = 4.5$ (Ref. [29])
HCHO/TPD	CO: traces, reduction to $CH_2{=}CH_2 = 87\%$ (this work)	CO: traces, reduction to $CH_3OH = 59\%$ (this work)	–

[a] $O_l^{2-} + 2Ce_l^{4+} \rightarrow (1/2)O_2(g) + V_0 + 2Ce_l^{3+}$.
[b] Calculated following the method given in Ref. [39].

surface as well as in the bulk. These H atoms will react with adsorbed formaldehyde making methanol (59%). On single crystal the small amounts of H atoms are provided from the total decomposition of HCHO (and some from the bulk that have diffused to the surface during TPD) have little effect on the reduction process. This allows HCHO to reductively couple to pinacolates [31] that leave the surface as ethylene (87%) putting extra O atoms on the surface. UO_2 can accommodate large amounts of excess O up to $UO_{2.25}$ in a superstructure (2:2:2) configuration [32]. We have previously found considerable formation of ethylene from formic acid over Ar^+-sputtered UO_2(1 1 1) and attributed this to reductive coupling of formaldehyde formed from formic acid [24]. This is also in line with results of higher aldehydes and ketones over reduced UO_2(1 1 1) single crystal where C4 and C6 hydrocarbons were formed from acetaldehyde [33] and acetone [34], respectively, by coupling reactions. Actually U is very active for the reductive coupling of aldehydes and ketones as evidenced by numerous works of organometallic chemists [35,36]. It was not possible however, in this work, to make the polycrystalline oxide active for this reaction because of the presence of excess H atoms. We are currently investigating the possibility of making small UO_2 clusters (by thermal decomposition of $(UO_2(CH_3COOH)_2{\cdot}2H_2O)$) on the surface of SiO_2 and TiO_2 as an alternative method for making polycrystalline UO_2 active for the reductive coupling reaction.

IR data show that adsorbed formaldehyde in the form of polyoxymethylene and dioxymethylene is oxidised by surface O to formates with increasing temperature. Making formate from dioxymethylene requires the removal of one H atom:

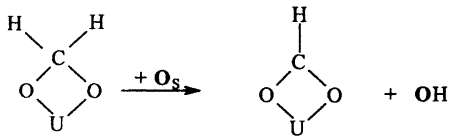

dioxymethylene formate

The insert in Fig. 7 shows the intensity of the ν_a(COO) of formates as function of $1/T$ when large amounts of adsorbed polyoxymethylene and dioxymethylene are present. The linearity is very good ($R^2 = 0.99$) and from the slope of the line an activation energy of ≈12 kJ/mol is computed. This can be related to that required for H abstraction from dioxymethylene to make formates.

In summary, the main reaction pathway of HCHO over UO_2(1 1 1) single crystal is coupling to $CH_2{=}CH_2$, while that on polycrystalline UO_2 (formed by H_2-reduction of α-U_3O_8) is reduction to methanol. IR analyses indicate that HCHO is adsorbed in a di- and polyoxymethylenic forms. A large fraction of these stable species leave the surface after hydrogenation as methanol. The remaining fraction is dehydrogenated to formates. From the intensity of ν_{as}(COO) of formates in the 250–450 K temperature domain an activation energy of 12 kJ/mol is computed for the dehydrogenation of dioxymethylene to formates. The decomposition of formates (mainly to CO_2) occurs at 600 K for both surfaces. The similarity between the main reaction product (CO_2) and reaction temperature (600 K) for formates decomposition over the single crystal and the polycrystalline surfaces of UO_2 indicates the absence of pressure and textural effects for the decomposition pathway.

Acknowledgements

S.D. Senanayake thanks RISIS PTE Ltd., Singapore, for granting a PhD scholarship.

References

[1] J.A. Lloyd, W.L. Manner, L.T. Paffett, Surf. Sci. 423 (1999) 265.
[2] B.E. Khan, R.D. Riecki, Chem. Rev. 88 (1988) 733.
[3] H. Madhavaram, H. Idriss, J. Catal. 206 (2002) 155.
[4] C.A. Colmenars, Prog. Solid State Chem. 9 (1974) 139.
[5] G.Ya. Popova, T.V. Andrushkevich, Yu.A. Chesalov, E.S. Stoyanov, Kinet. Catal. 41 (2000) 885, and references therein.
[6] H. Idriss, M.A. Barteau, Surf. Sci. 262 (1992) 113.
[7] G.Ya. Popova, Yu.A. Chesalov, T.V. Andrushkevich, I.I. Zakharov, E.S. Stoyanov, J. Mol. Catal. A 158 (2000) 345.
[8] H. Idriss, J.P. Hindermann, R. Kieffer, A. Kiennemann, A. Vallet, C. Chauvin, J.C. Lavalley, P. Chaumette, J. Mol. Catal. 42 (1997) 205.
[9] A. Kiennemann, H. Idriss, R. Kieffer, P. Chaumette, D. Durand, Ind. Eng. Chem. Res. 30 (1991) 1130.
[10] G. Busca, J. Lamotte, J.C. Lavalley, V. Lorenzelli, J. Am. Chem. Soc. 109 (1987) 5197.
[11] C. Li, K. Domen, K.-I. Maruya, T. Onishi, J. Catal. 125 (1990) 445.

[12] M. Ai, J. Catal. 83 (1983) 141.
[13] R.C. Wall, Chevron Research Co., US Patent 4 144 401 (1979).
[14] G. Lu, A. Linsbigler, J.T. Yates, J. Phys. Chem. 99 (1995) 7626.
[15] T.J.A. Mazanec, J. Catal. 98 (1986) 115.
[16] K. Tanabe, K. Saito, J. Catal. 35 (1974) 247.
[17] P.W. Tasker, Surf. Sci. 78 (1979) 315.
[18] S.V. Chong, T.R. Griffith, H. Idriss, Surf. Sci. 444 (2000) 187.
[19] E.I. Ko, J.B. Benziger, R.J. Madix, J. Catal. 62 (1980) 264.
[20] T. Meichel, J. Suzanne, C. Girard, C. Girardet, Phys. Rev. B 38 (1988) 3781.
[21] H. Madhavaram, P. Buchanan, H. Idriss, J. Vac. Sci. Technol. A 15 (1997) 1685.
[22] A. Yee, S.J. Morrison, H. Idriss, J. Catal. 191 (2000) 30.
[23] P.-Y. Sheng, A. Yee, G.A. Bowmaker, H. Idriss, J. Catal. 208 (2002) 393.
[24] S.V. Chong, H. Idriss, Surf. Sci. 504 (2002) 145.
[25] T. Shimanoushi, Tables of Molecular Vibrational Frequencies Consolidated, vol. 1, National Bureau of Standard, 1972, pp. 1–160. http://www.webbook.nist.gov.
[26] A.B. Anton, J.E. Parmeter, W.H. Weinberg, J. Am. Chem. Soc. 108 (1986) 1823.
[27] H. Tadokoro, M. Kobayashi, Y. Kawagushi, A. Kobayashi, S. Murahashi, J. Chem. Phys. 38 (1963) 703.
[28] W.S. Sim, P. Gardner, D.A. King, J. Phys. Chem. 100 (1996) 12509.
[29] J. Stubernrauch, E. Brosha, J.M. Vohs, Catal. Today 28 (1996) 431.
[30] E. Spinner, J. Chem. Soc. (1964) 4217.
[31] K.T. Queeney, C.R. Arumainayagam, A. Balaji, C.M. Friend, Surf. Sci. 418 (1998) L31.
[32] R.J. Tilley, Defect Crystal Chemistry, Blackie, Glasgow, London, 1986.
[33] S.V. Chong, H. Idriss, J. Vac. Sci. Technol. A 19 (2001) 1933.
[34] S.V. Chong, Ph.D. Thesis, University of Auckland, 2001.
[35] C. Villiers, M. Epheritikhine, Chem. Eur. J. 7 (2001) 304.
[36] O. Maury, C. Villiers, M. Epheritikhine, Angew. Chem. 108 (1996) 1215.
[37] J.L. Davis, M.A. Barteau, J. Am. Chem. Soc. 111 (1989) 1782.
[38] T.X.T. Sayle, S.C. Parker, C.R.A. Parker, Surf. Sci. 316 (1994) 329.
[39] H. Idriss, M.A. Barteau, Adv. Catal. 45 (2000) 261 (equation given in page 307).
[40] C.R.A. Catlow, J. Chem. Faraday Trans. II 74 (1978) 1901.
[41] J.Q. Broughton, P.S. Bagus, J. Electr. Spec. Relat. Phenom. 20 (1980) 261.
[42] S.D. Senanayake, H. Idriss, Stud. Surf. Sci. Catal., in press.